Proceedings of the 3rd International Conference on Mechatronics and Smart Systems
DOI: 10.54254/2755-2721/2025.24802

Design of an IMU-Based Non-Invasive Registration System for Navigation in Total Hip Arthroplasty (THA)

Shaojie Su[1*], Yangsheng Chen[1], Zhenwei Wei[1], Jiasheng Cai[1], Zhaofeng Lin[2]

[1]*School of Information Engineering, Fujian Business University, Fuzhou, China*
[2]*Department of Surgery, Traditional Chinese Medicine Hospital, Quanzhou, China*
**Corresponding Author. Email: susj12@tsinghua.org.cn*

Abstract. Accurate acetabular cup placement in total hip arthroplasty (THA) requires reliable registration to establish body-to-world coordinate transformation, yet traditional methods rely on bony landmarks or invasive pins. This paper presents an inertial measurement unit (IMU)-based registration system for THA without bony landmark reliance or invasive contact. The system hardware integrates a 3-axis accelerometer and a 3-axis gyroscope as a sensor module, with Extended Kalman Filter (EKF) applied for motion data fusion. The software employs a rotation matrix and Euler angle combined registration algorithm to compute coordinate transformations. Experiments using a 3-axis tilt table validate the IMU's angle estimation accuracy (RMSE 0.400°–0.423°) and the robust acquisition of rotation axis vectors during registration. Although it is theoretically and experimentally feasible, the registration relies on the assumption of patient–operating table immobility. Pending further optimization and clinical validation, this portable, cost-effective, and radiation-free solution shows potential as a standard registration tool for THA navigation devices.

Keywords: THA, registration, IMU, navigation, safe zone.

1. Introduction

With the aging population, the demand for total hip arthroplasty (THA) has grown significantly due to increasing hip joint disorders [1]. THA is the primary procedure to restore mobility, with over half a million surgeries annually in the U.S. alone [2]. As shown in Figure 1, the THA procedure comprises three steps, with the step 2 being the most citical: the success of THA largely depends on implanting the acetabular cup into the "safe zone" [3], which was first proposed by Lewinnek et al. in 1978 [4], defining optimal cup placement angles for THA: 40°±10° inclination and 15°±10° anteversion. Improper placement leads to complications like dislocation and prosthetic failure [5].

© 2025 The Authors. This is an open access article distributed under the terms of the Creative Commons Attribution License 4.0 (https://creativecommons.org/licenses/by/4.0/).

DOI: 10.54254/2755-2721/2025.24802



Figure 1: Overview of the three steps in the THA procedure

Many methods help determine intraoperative cup placement. Mechanical alignment guides (MAGs) are common and affordable, but rely heavily on surgeons' experience [6]. Protractors are more precise but suit only preoperative planning or simple cases [7]. Computer/robot-assisted systems are the most accurate but are complex and costly, and they increase preoperative radiation exposure and require bone markers, causing extra bone damage and higher pin-tract complication risks [8], [9]. Inertial measurement unit (IMU)-based inclinometers offer real-time, radiation-free intraoperative guidance but still require bony pins for registration, which can cause the risk of pin site complications [10], [11].

Among these methods for THA, registration is an essential step as it establishes the relationship between the patient's body coordinate system and the world coordinate system. In this paper, we introduce an IMU-based registration system, aiming to assist surgeons using navigation devices in establishing the patient's body to world coordinate transformation without reliance on bony landmarks or invasive contact. It is a real-time, radiation-free, portable, and cost-effective solution.

2. System design

2.1. Problem definition

Acetabular cup inclination and anteversion, which determine the placement safe zone, are two angles defined in the human body coordinate system as shown in Figure 2(a). Since navigation devices can only directly get the orientations of surgical tools and implants relative to the world coordinate system, we need a registration system to first set up the body-to-world coordinate transformation, which is solved in this paper. Then the navigation devices can check if the implant is in the safe zone.

To mathematically achieve registration, three coordinate systems need to be defined first. The body system {B} is built using the coronal, sagittal, and horizontal planes of the human body as shown in Figure 2(b), with its positive x-axis orthogonal to the sagittal plane and pointing to the body's right, the positive y-axis orthogonal to the coronal plane and pointing forward, and the positive z-axis as the vertical upward direction along the spinal axis. Meanwhile, the East-North-Up (ENU) system is used as the definition of the world system {W}, while a body-fixed coordinate system on the sensor is used as the IMU system {I}, as shown in Figure 3.

DOI: 10.54254/2755-2721/2025.24802

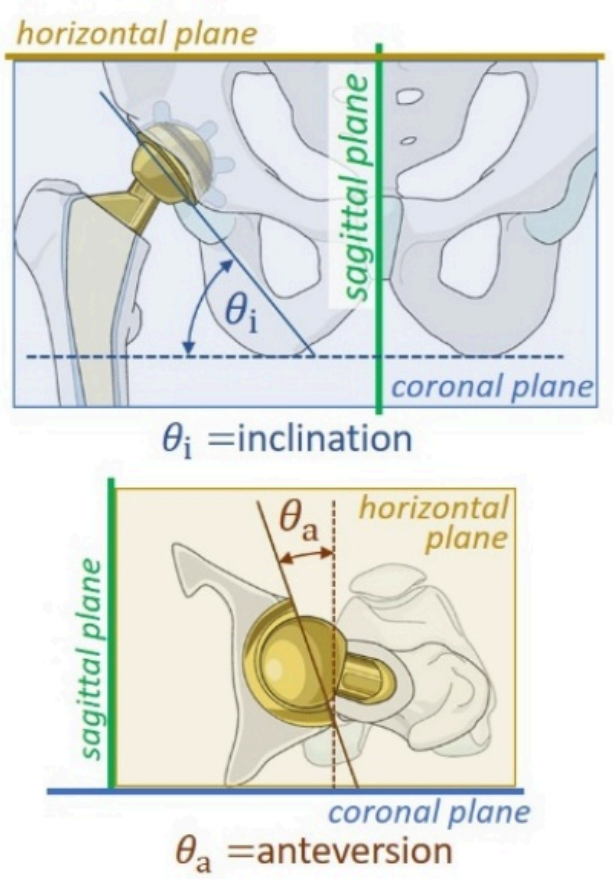

(a) Definition of inclination and anteversion

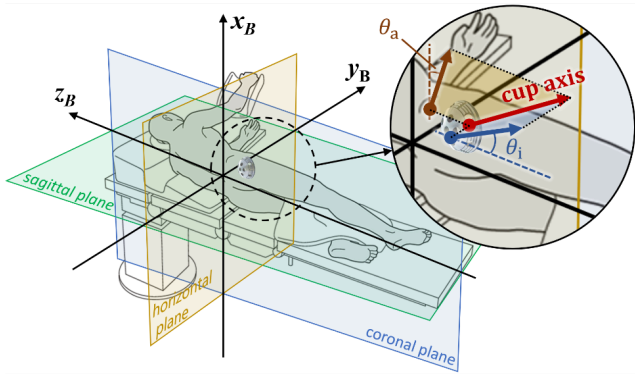

(b) Definition of human body coordinate system {B} and illustration of cup axis and θ_i, θ_a.

Figure 2: Registration aims to establish the body-to-world coordinate transformation

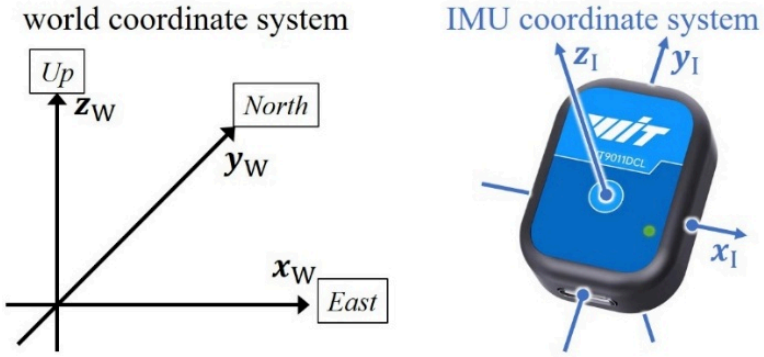

Figure 3: Definitions of the world coordinate system {W} and the IMU coordinate system {I}

2.2. System architecture

The registration system architecture consists of two interconnected components: hardware and software, as illustrated in Figure. 4. The hardware captures motion data and fuses them through an Extended Kalman Filter (EKF), then wirelessly transmits them to the software side through Bluetooth. The PC processor executes the registration algorithm to establish the body-to-world

DOI: 10.54254/2755-2721/2025.24802

coordinate transformation and finally passes it as parameters to the navigation device for further pose estimation.

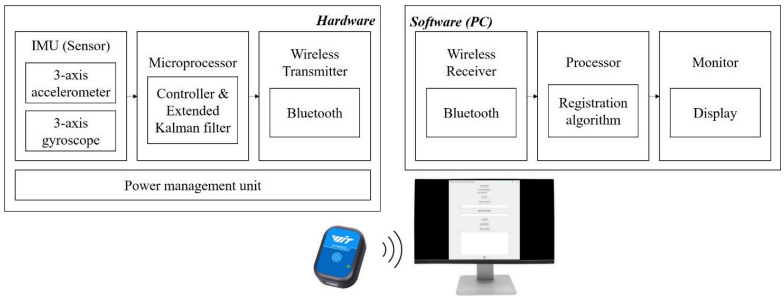

Figure 4: Architecture of the IMU-based registration system

3. Methods

3.1. Transformation between coordinate systems

Rotation matrices and Euler angles are fundamental tools for describing the rotation of a rigid body [12]. In this paper, the Euler angles known as Tait-Bryan angles (yaw, pitch and roll) are used, which decompose the rotation into intrinsic-type rotations with the order of z-y-x. Extrinsic rotations refer to rotations that are applied to a space-fixed coordinate system, while intrinsic rotations involve applying each rotation about the axes of the current coordinate system (also known as a body-fixed coordinate system) [13]. For a set of Euler angles (α, β, γ) acquired from the IMU, the net rotation $\boldsymbol{R}_{\mathrm{I}}^{\mathrm{W}}$ is expressed as (1), where c_α and s_α are short for $\cos\alpha$ and $\sin\alpha$, respectively.

$$\boldsymbol{R}_{\mathrm{I}}^{\mathrm{W}} = \boldsymbol{R}_z(\gamma)\boldsymbol{R}_y(\beta)\boldsymbol{R}_x(\alpha) = \begin{bmatrix} \mathrm{c}_\beta\mathrm{c}_\gamma & \mathrm{s}_\alpha\mathrm{s}_\beta\mathrm{c}_\gamma - \mathrm{c}_\alpha\mathrm{s}_\gamma & \mathrm{c}_\alpha\mathrm{s}_\beta\mathrm{c}_\gamma + \mathrm{s}_\alpha\mathrm{s}_\gamma \\ \mathrm{c}_\beta\mathrm{s}_\gamma & \mathrm{s}_\alpha\mathrm{s}_\beta\mathrm{s}_\gamma + \mathrm{c}_\alpha\mathrm{c}_\gamma & \mathrm{c}_\alpha\mathrm{s}_\beta\mathrm{s}_\gamma - \mathrm{s}_\alpha\mathrm{c}_\gamma \\ -\mathrm{s}_\beta & \mathrm{s}_\alpha\mathrm{c}_\beta & \mathrm{c}_\alpha\mathrm{c}_\beta \end{bmatrix} \tag{1}$$

In addition to describing rotational movement, the rotation matrix $\boldsymbol{R}_{\mathrm{I}}^{\mathrm{W}}$ also represents the coordinate transformation relationship from {I} to {W}. Assuming $\boldsymbol{p}^{\mathrm{W}}$ denotes the coordinates of a fixed vector $\boldsymbol{p}$ in {W}, and $\boldsymbol{p}^{\mathrm{I1}}$ and $\boldsymbol{p}^{\mathrm{I2}}$ denote the coordinates in {I} of the IMU's first and second attitude, respectively, the relationships of these coordinates can be expressed as (2).

$$\boldsymbol{p}^{\mathrm{W}} = \boldsymbol{R}_{\mathrm{I1}}^{\mathrm{W}}\boldsymbol{p}^{\mathrm{I1}} = \boldsymbol{R}_{\mathrm{I1}}^{\mathrm{W}}\boldsymbol{R}_{\mathrm{I2}}^{\mathrm{I1}}\boldsymbol{p}^{\mathrm{I2}} = \boldsymbol{R}_{\mathrm{I2}}^{\mathrm{W}}\boldsymbol{p}^{\mathrm{I2}} \tag{2}$$

3.2. Registration algorithm

Assuming that the patient and the operating table maintain relative immobility throughout the surgery, the operating table's orientation is used to represent the patient's body (e.g., left lateral decubitus shown in Figure 2(b)). The IMU is mounted on the operating table, which is then rotated about its long axis (i.e., z_{B}-axis) by a small angle (about 10°). By recording the Euler angles $(\alpha_1, \beta_1, \gamma_1)$ and $(\alpha_2, \beta_2, \gamma_2)$ from the IMU before and after rotation, the relative transformation can be derived as (3).

DOI: 10.54254/2755-2721/2025.24802

$$\boldsymbol{R}_{\mathrm{I2}}^{\mathrm{I1}}=\boldsymbol{R}_{\mathrm{I1}}^{\mathrm{W}-1}\boldsymbol{R}_{\mathrm{I2}}^{\mathrm{W}}=\boldsymbol{R}_{\mathrm{I1}}^{\mathrm{W}\mathrm{T}}\boldsymbol{R}_{\mathrm{I2}}^{\mathrm{W}}=\boldsymbol{R}_{x}^{\mathrm{T}}\left(\alpha_{1}\right)\boldsymbol{R}_{y}^{\mathrm{T}}\left(\beta_{1}\right)\boldsymbol{R}_{z}^{\mathrm{T}}\left(\gamma_{1}\right)\boldsymbol{R}_{z}\left(\gamma_{2}\right)\boldsymbol{R}_{y}\left(\beta_{2}\right)\boldsymbol{R}_{x}\left(\alpha_{2}\right) \tag{3}$$

Convert $\boldsymbol{R}_{\mathrm{I2}}^{\mathrm{I1}}$ into the axis/angle representation as a unit vector $\boldsymbol{u}=\left(u_{x},\,u_{y},\,u_{z}\right)^{\mathrm{T}}$ along the rotation axis and a counterclockwise rotation angle φ about this axis as shown in (4), where $\mathrm{tr}\left(\boldsymbol{R}_{\mathrm{I2}}^{\mathrm{I1}}\right)$ denotes the trace of $\boldsymbol{R}_{\mathrm{I2}}^{\mathrm{I1}}$, while $\boldsymbol{R}_{\mathrm{I2}}^{\mathrm{I1}}\left(\mathrm{i},\mathrm{j}\right)$ represents the element in its i-th row and j-th column.

$$\begin{cases}\cos\varphi=\frac{1}{2}\left[\mathrm{tr}\left(\boldsymbol{R}_{\mathrm{I2}}^{\mathrm{I1}}\right)-1\right]\\ \sin\varphi=\sqrt{1-\cos^{2}\varphi}\end{cases},\quad\begin{cases}u_{x}=\frac{1}{2\sin\varphi}\left[\boldsymbol{R}_{\mathrm{I2}}^{\mathrm{I1}}\left(3,2\right)-\boldsymbol{R}_{\mathrm{I2}}^{\mathrm{I1}}\left(2,3\right)\right]\\ u_{y}=\frac{1}{2\sin\varphi}\left[\boldsymbol{R}_{\mathrm{I2}}^{\mathrm{I1}}\left(1,3\right)-\boldsymbol{R}_{\mathrm{I2}}^{\mathrm{I1}}\left(3,1\right)\right]\\ u_{z}=\frac{1}{2\sin\varphi}\left[\boldsymbol{R}_{\mathrm{I2}}^{\mathrm{I1}}\left(2,1\right)-\boldsymbol{R}_{\mathrm{I2}}^{\mathrm{I1}}\left(1,2\right)\right]\end{cases} \tag{4}$$

Since $\boldsymbol{R}_{\mathrm{I2}}^{\mathrm{I1}}$ is an intrinsic-type rotation matrix, the coordinates of $\boldsymbol{u}$ (i.e., the unit vector $\boldsymbol{e}_{\mathrm{B}z}$ of the z_B-axis) are in {I} before rotation, and can be transformed to {W} as shown in (5) using $\boldsymbol{R}_{\mathrm{I1}}^{\mathrm{W}}$. Meanwhile, as the operating table is horizontally placed, the x_B-axis is considered parallel to the z_W-axis, meaning that the coordinates of the unit vector $\boldsymbol{e}_{\mathrm{B}x}$ and $\boldsymbol{e}_{\mathrm{B}y}$ can be represented as (6) and (7).

$$\boldsymbol{e}_{\mathrm{B}z}^{\mathrm{W}}=\boldsymbol{u}^{\mathrm{W}}=\boldsymbol{R}_{\mathrm{I1}}^{\mathrm{W}}\boldsymbol{e}_{\mathrm{B}z}^{\mathrm{I1}}=\boldsymbol{R}_{\mathrm{I1}}^{\mathrm{W}}u \tag{5}$$

$$\boldsymbol{e}_{\mathrm{B}x}^{\mathrm{W}}=\boldsymbol{e}_{\mathrm{W}z}^{\mathrm{W}}=\left(0,\,0,\,1\right)^{\mathrm{T}} \tag{6}$$

$$\boldsymbol{e}_{\mathrm{B}y}^{\mathrm{W}}=\boldsymbol{e}_{\mathrm{B}z}^{\mathrm{W}}\times\boldsymbol{e}_{\mathrm{B}x}^{\mathrm{W}} \tag{7}$$

According to the definition of the rotation matrix, the transformation matrix $\boldsymbol{R}_{\mathrm{B}}^{\mathrm{W}}$ can be finally expressed as shown in (8), where $\boldsymbol{e}_{\mathrm{B}x}^{\mathrm{B}}$, $\boldsymbol{e}_{\mathrm{B}y}^{\mathrm{B}}$ and $\boldsymbol{e}_{\mathrm{B}z}^{\mathrm{B}}$ are the coordinates of the orthonormal basis vectors of {B} in its own system, meaning that the matrix $\left[\boldsymbol{e}_{\mathrm{B}x}^{\mathrm{B}}\quad\boldsymbol{e}_{\mathrm{B}y}^{\mathrm{B}}\quad\boldsymbol{e}_{\mathrm{B}z}^{\mathrm{B}}\right]$ is an identity matrix.

$$\boldsymbol{R}_{\mathrm{B}}^{\mathrm{W}}=\boldsymbol{R}_{\mathrm{B}}^{\mathrm{W}}\left[\boldsymbol{e}_{\mathrm{B}x}^{\mathrm{B}}\quad\boldsymbol{e}_{\mathrm{B}y}^{\mathrm{B}}\quad\boldsymbol{e}_{\mathrm{B}z}^{\mathrm{B}}\right]=\left[\boldsymbol{e}_{\mathrm{B}x}^{\mathrm{W}}\quad\boldsymbol{e}_{\mathrm{B}y}^{\mathrm{W}}\quad\boldsymbol{e}_{\mathrm{B}z}^{\mathrm{W}}\right] \tag{8}$$

With the relationship $\boldsymbol{R}_{\mathrm{B}}^{\mathrm{W}}$ established, the registration is completed. It requires no body markers and is independent of bony landmarks. However, it relies on the assumption of patient–table immobility, so proper patient positioning and table leveling are critical for successful registration.

4. Experiments and results

A 3-axis tilt table is used to validate the effectiveness of the IMU-based registration system, as shown in Figure 5. This precision instrument consists of three layers, with a main scale and a vernier sub-scale equiped at each layer to achieve a resolution of 0.1°. A threaded rod with an acetabular cup attached at the end is vertically screwed into the center to simulate the cup axis during surgery.

DOI: 10.54254/2755-2721/2025.24802

4.1. Angle estimation accuracy experiment

This experiment aimed to test the IMU's fundamental functionality of angle estimation. The tilt table with an IMU mounted on it was directed to perform a series of rotations about the three axes. The angle values from the tilt table (true values) and those computed from the IMU (estimated values) were compared as shown in Figure 6(a). The results demonstrated that, the estimated angles were in good agreement with the true ones. The absolute errors stayed within ±1° and the root mean square error (RMSE) ranged from 0.400° to 0.423°, which is well within the clinical tolerance of safe zone.

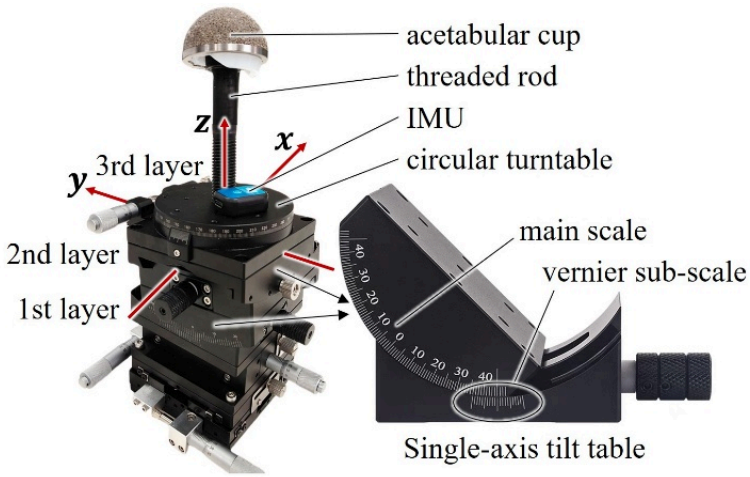

Figure 5: The full view of the 3-axis tilt table used for experiments

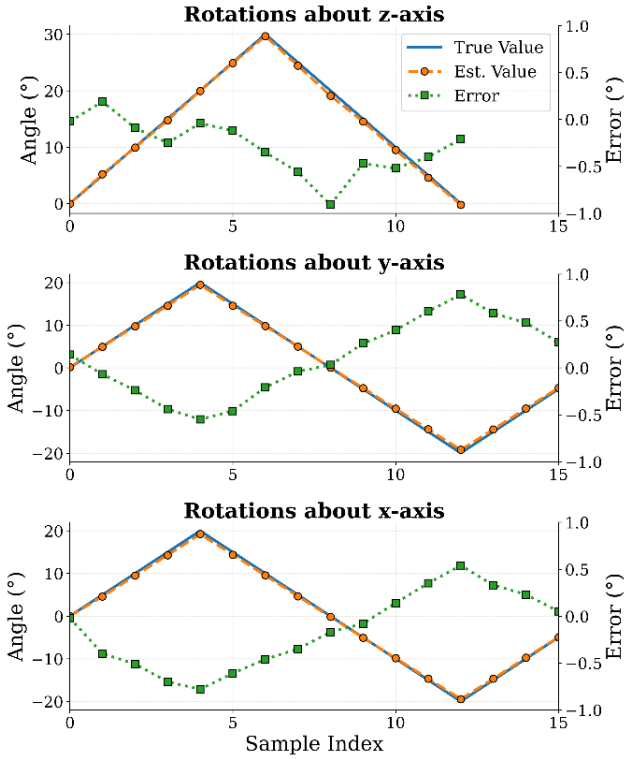

(a) Comparison of true and estimated rotational angles about the three axes

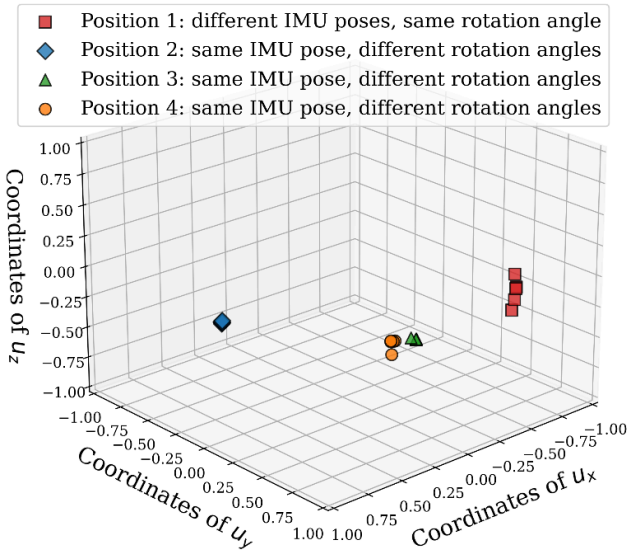

(b) Coordinates of rotation axis unit vector $\boldsymbol{u}^{\mathrm{W}}$ in {W} acquired during registration

DOI: 10.54254/2755-2721/2025.24802

Figure 6: Results of experiments conducted using the 3-axis tilt table

4.2. Rotation axis acquisition experiment

Registration depends on accurately acquiring the rotation axis vector. So in this experiment, the tilt table with the IMU mounted on its turntable was positioned at four different locations and was rotated about its y-axis to simulate the operating table's rotation about its long axis during registration, and our algorithm was to estimate the coordinates of the unit vector along this rotation axis. Results under different conditions are plotted in a scatter plot as shown in Figure 6(b). Since the tilt table sits on the test table, its y-axis almost remains horizontal, meaning the values of u_z^{W} should be close to zero, with only u_x^{W} and u_y^{W} changing across different positions. Among all 20 tests, only 4 showed minor anomalies where $|u_z^{\mathrm{W}}| > 0.1$ (likely caused by noise), while the remaining had $|u_z^{\mathrm{W}}|$ within 0.04.

5. Conclusion

This paper presents an IMU-based registration system for THA, designed to establish the body-to-world coordinate transformation for navigation devices without relying on bony landmarks or invasive contact. By integrating a 3-axis accelerometer, gyroscope, and Extended Kalman Filter (EKF) in the hardware module, and a rotation matrix-Euler angle combined registration algorithm in the software, the system achieves real-time, radiation-free navigation support.

Experimental results demonstrate that the IMU provides angle estimation with RMSE ranging from 0.400° to 0.423°, which is much better than the safe zone tolerance. The reliability of the registration algorithm is also validated as it successfully acquires the body coordinate system's axis vectors with high consistency. This portable and cost-effective solution has the potential to become a standard registration tool for assisting navigation device setup in THA, pending further optimization and clinical validation.

Acknowledgement

This work was supported by the Fujian Provincial Natural Science Foundation (No. 2021J01335).

References

[1] Thomas, B. J., & Stiehl, J. B. (2004). Basic of total hip replacement surgery. Navigation and Robotics in Total Joint and Spine Surgery, Springer Berlin Heidelberg.
[2] Siddiqi, A., Levine, B. R., & Springer, B. D. (2022). Highlights of the 2021 american joint replacement registry annual report. Arthroplasty today, 13, 205-207.
[3] Sadhu, Anita, Denis, Coobs, Benjamin, R., & Barrack, et al. (2017). Acetabular Component Position and the Risk of Dislocation Following Primary and Revision Total Hip Arthroplasty: A Matched Cohort Analysis. J Arthroplasty, 32(3): 987-991.
[4] Lewinnek, G. E., Lewis, J. L., Tarr, R., et al. (1978). Dislocations after total hip-replacement arthroplasties. Journal of Bone & Joint Surgery, 60(2), 217-220.
[5] Nutt, J. L., Papanikolaou, K., & Kellett, C. F. (2013). (ii) complications of total hip arthroplasty. Orthopaedics & Trauma, 27(5), 272-276.
[6] Duren, B. H. V., Royeca, J. M., Cunningham, C. M., Lamb, J. N., Brew, C. J., & Pandit, H. (2021). Can the use of an inclinometer improve acetabular cup inclination in total hip arthroplasty? a review of the literature. SAGE Publications, (5).
[7] Maillot, Cédric, Harman, C., Villet, Loïc, Cobb, J., & Rivière, Charles. (2019). Modern cup alignment techniques in total hip arthroplasty: a systematic review. Orthopaedics & Traumatology Surgery & Research.

DOI: 10.54254/2755-2721/2025.24802

[8] Miura, T., Yamamoto, N., Shiroshita, A., Tsuge, T. P., Saitsu, A., & Yoshitani, J., et al. (2024). Comparison of implant placement accuracy between manual, robot-assisted, computer-navigated, augmented reality navigated, patient-specific instrumentation, and accelerometer navigated total hip arthroplasty: a systematic review and network meta-analysis. JBJS Review, 12(11), 12.
[9] Ryan, J. A., Jamali, A. A., & Bargar, W. L. (2010). Accuracy of computer navigation for acetabular component placement in tha. Clinical Orthopaedics and Related Research®, 468(1), 169-177.
[10] Darrith, B., Bell, J. A., & Culvern, C. D. V. C. J. (2018). Can the use of an inclinometer improve the positioning of the acetabular component in total hip arthroplasty? The bone & joint journal, 100/B(7), 862-866.
[11] O'Neill Christopher K J, Hill, J. C., Patterson, C. C., Molloy, D. O., Gill, H. S., & Beverland, D. E. (2018). Reducing variability in apparent operative inclination during total hip arthroplasty: findings of a randomised controlled trial. HIP International, 28(3), 234-239.
[12] Siciliano, B., Sciavicco, L., Villani, L., & Oriolo, G. (2011). Robotics: Modelling, Planning and Control. Springer.
[13] Markley, F. L., & Crassidis, J. L. (2014). Fundamentals of Spacecraft Attitude Determination and Control. Springer New York.